Research Article

Journal of Geophysical Research: Oceans
DOI 10.1002/2016JC011807

Quantifying the residual volume transport through a multiple-inlet system in response to wind forcing: the case of the western Dutch Wadden Sea

Matias Duran-Matute[1,2], **Theo Gerkema**[2], **Maximiliano G. Sassi**[2]

[1]Department of Applied Physics, Eindhoven University of Technology, Eindhoven, The Netherlands.

[2]NIOZ Royal Netherlands Institute for Sea Research, Department of Estuarine and Delta Systems, and Utrecht University, Yerseke, The Netherlands.

Corresponding author: M. Duran-Matute, m.duran.matute@tue.nl

Received: Mar 19, 2016; Revised: Oct 05, 2016; Accepted: Nov 15, 2016

Abstract

In multiple-inlet coastal systems like the western Dutch Wadden Sea, the tides (and their interaction with the bathymetry), the fresh water discharge, and the wind drive a residual flow through the system. In the current paper, we study the effect of the wind on the residual volume transport through the inlets and the system as a whole on both the short (one tidal period) and long (seasonal or yearly) time scales. The results are based on realistic three-dimensional baroclinic numerical simulations for the years 2009-2011. The length of the simulations (over 2000 tidal periods) allowed us to analyze a large variety of conditions and quantify the effect of wind on the residual volume transport. We found that each inlet has an anisotropic response to wind; i.e. the residual volume transport is much more sensitive to the wind from two inherent preferential directions than from any other directions. We quantify the effects of wind on the residual volume transport through the system and introduce the concept of the system's conductance for such wind driven residual transport. For the western Dutch Wadden Sea, the dominant wind direction in the region is close to the direction with the highest conductance and opposes the tidally driven residual volume transport. This translates in a large variability of the residual volume transport and a dominance of the wind in its long-term characteristics in spite of the episodic nature of storms.

1 Introduction

In multiple-inlet coastal lagoons, there is a net residual volume transport of water through the system. In other words, when averaging out the tidal currents, there is a residual inflow through some inlets and a residual outflow through others. This residual transport has been computed from measurements or numerical simulations in several multiple-inlet coastal lagoons like the Venice Lagoon (Italy) [*Bellafiore et al.*, 2008], the Wadden Sea (The Netherlands, Germany, and Denmark)[*Ridderinkhof*, 1988a; *Stanev et al.*, 2003; *Duran-Matute et al.*, 2014], the Ria Formosa Lagoon (Portugal) [*Salles et al.*, 2005; *Farinha Fabiao et al.*, 2016], and many found along the coast of the U.S.A. like several stretches of Florida's Intracoastal waterway [*Smith*, 1990; *Waterhouse et al.*, 2013], Tampa Bay (Florida) [*Meyers et al.*, 2007], the Albemarle-Pamlico Sound (South Carolina) [*Jia and Li*, 2012], and the Altamaha River Estuary, Sapelo Sound and Doboy Sound system (Georgia) [*Li*, 2013]. The interest on the residual volume transport arises from its effect on the long-term exchange of, for example, nutrients and pollutants between the coastal lagoon and the adjacent open sea, and hence, its impact on the overall ecology of the lagoon.

The residual volume transport through a coastal lagoon is jointly driven by the tides (and their interaction with the bathymetry), the fresh water discharged into the system, density gradients, and wind [see e.g. *Nihoul and Ronday*, 1975; *Buijsman and Ridderinkhof*, 2007]. The

tides can drive the residual volume transport due to differences in the tidal amplitude and phase and a difference in the residual sea surface height between the inlets [*van de Kreeke and Cotter*, 1974; *van de Kreeke*, 1976; *Liu and Aubrey*, 1993] and via nonlinear interaction between tides and topography [*Zimmerman*, 1981]. In reality, when all mechanism are active, the relevance of each of them depends in a complex way on the system and on the particular conditions during the given tidal period.

Wind has been shown to be able to force a residual volume transport that is much larger than the one forced by the tides. In fact, it acts as the main driver of the variability of the residual volume transport in many coastal lagoons, for example, in the Indian River Lagoon (Florida, U.S.A.) [*Smith*, 1990], for the two main inlets of the western Dutch Wadden Sea (WDWS) [*Buijsman and Ridderinkhof*, 2007]; in an idealized three-inlet system with a straight coast and the three straight channels perpendicular to the coast [*Li*, 2013]; in the Arcachon Lagoon (France) [*Salles et al.*, 2015]; and in the East Frisian Wadden Sea (EFWS) [*Herrling and Winter*, 2015]. Hence, the question arises of how to describe and quantify the effect of wind on the residual volume transport in multiple inlet systems as a function of both wind speed and direction.

This quantification is particularly challenging due to the complex geometry of the systems, the different orientation of the inlets, the different amplitudes and phases of the tide at each inlet for every given tidal period, and the variability in the wind, and the freshwater discharge. Simplifications have then been used in previous numerical and semi-analytical studies, for example, neglecting smaller inlets or watersheds (also known as *tidal divides*) *Buijsman and Ridderinkhof* [e.g. 2007], using vertically averaged simulations neglecting baroclinic effects and freshwater inflows [e.g. *Herrling and Winter*, 2015], considering simplified geometries *Li* [e.g. 2013], or modelling a small number of tidal cycles [e.g. *Stanev et al.*, 2003]. Observational studies, on the other hand, have shortcomings such as relatively short time span, temporal gaps, or limited spatial coverage [*Gerkema et al.*, 2014; *Salles et al.*, 2015; *Sassi et al.*, 2015a].

Figure 1. Map of the Dutch Wadden Sea. The names of the islands, inlets and the two main sluices are indicated. The color denotes the depth. The red lines denotes the transects across the three first inlets and the Terschelling watershed at which data were extracted.

In the western Dutch Wadden Sea, the magnitude of residual volume transport driven by tides alone was estimated to be about 1000 $m^3\ s^{-1}$ flowing mainly from the Vlie Inlet to the Texel Inlet [*Ridderinkhof*, 1988a,b]. In reality, this value can vary slightly depending on the tidal conditions (spring-neap cycle, daily inequality) and even more by the effect of wind:

large residual volume transport coincide with strong wind events particularly from the South-west [*Buijsman and Ridderinkhof*, 2007; *Duran-Matute et al.*, 2014]. However, the link between wind and the residual volume transport has previously neither been shown in a statistical sense nor quantified.

In the current paper, we provide a full description and quantification of the effect of wind on the residual volume transport through the WDWS (see Fig. 1) while taking into consideration all of the complexity that state-of-the-art numerical simulations allow, i.e. using three-dimensional baroclinic numerical simulations with a realistic bathymetry, a high resolution, a drying-and-flooding algorithm, and realistic forcing that includes tides, wind surges, wind, freshwater discharge, and atmospheric forcing. The simulations span three full years (2009-2011). This translates in over 2000 tidal periods with a large variety and range of forcing conditions that allow us to quantify the effect of wind on the residual volume transport through the system both in the short-term (one tidal period) and the long term (seasonal and yearly). More generally, we outline a method to extract the relevant information and quantify the sensitivity of the residual volume transport to both wind direction and speed. With this, it is possible to predict, within a relatively small margin of error, the residual volume transport through the WDWS when the wind conditions are known.

We additionally address questions related to the long term effect of wind: Can sporadic strong wind events have an effect on the long term (e.g. yearly) flushing of the system? Are there certain average wind conditions that could further promote this long-term flushing? These questions are relevant in view of the decadal variability in the dominant wind direction and the occurrence and intensity of storms [see e.g. *Weisse et al.*, 2012; *Smits et al.*, 2005].

The rest of this paper is organized as follows. In Sec. 2, we describe the study area and the characteristics of the wind in the region. Section 3 describes the numerical setup and the method to calculate tidally average quantities, and discusses the validation of the numerical results. In Sec. 4, we describe the effect of the wind on the tidally averaged set-ups and set-downs inside the western Dutch Wadden Sea, and in Sec. 5 we describe the effect of the wind on the tidally averaged residual volume transport. Sec. 6 is devoted to the discussion of the long term effects the wind has on the residual volume transport. Finally, the conclusions are outlined in Sec. 7.

2 Study Area

2.1 Geographical Location

The western Dutch Wadden Sea (WDWS), also known as the Marsdiep-Vlie basin, covers an area of about 1500 km^2 and holds an average volume of $4.75{\cdot}10^9$ m^3. It is a meso-tidal

estuary with a tide range slightly larger than 2 m dominated by the semidiurnal M2 component.

The WDWS is connected to the North Sea by three tidal inlets. These are, from West to East, the Texel inlet, the Eierlandse Gat, and the Vlie inlet (Figure 1). The WDWS is connected to the Eastern Dutch Wadden Sea (EDWS) through the Terschelling watershed (also referred to as *tidal divide*). In terms of their cross-sectional area, the Texel inlet has a size of $55{\cdot}10^3$ m^2 at the transect depicted in Figure 1. The Vlie inlet, being overall broader but with a narrower main channel, has a similar cross-sectional area, $61{\cdot}10^3$ m^2, while the Eierlandse Gat is significantly smaller ($15{\cdot}10^3$ m^2). Further into the basin, the main channel of each inlet bifurcates into smaller ones. For the shallow watershed south of Terschelling, the cross-sectional area is the smallest ($12.5{\cdot}10^3$ m^2 with respect to mean sea level). In this case, the actual cross-sectional area at any given moment depends strongly on the water level, which is on average less than 1 m above the bottom.

In terms of their tidal prism, the Texel inlet and the Vlie inlet are of similar importance ($\sim 10^9$ m^3), while the Eierlandse Gat has a much smaller one ($\sim 1.8{\cdot}10^8$ m^3) [*Louters and Gerritsen*, 1994; *Duran-Matute et al.*, 2014]. Although the tidal prism through the Terschelling watershed is the smallest ($\sim 3.3 \cdot 10^7$ m^3), the residual volume transport is similar to that through the major inlets [*Duran-Matute et al.*, 2014].

The WDWS has two main sources of freshwater: the sluices of Den Oever and Kornwerderzand located at the closing dike separating the Wadden Sea from Lake IJssel, a freshwater lake. The average fresh water discharge from these two sluices was 428 m^3 s^{-1} for the period 2009-2011, and it accounted for 96% of the fresh water discharged into the WDWS from all the sluices around it.

In spite of their connection through the Terschelling watershed, the WDWS and the EDWS have traditionally been considered as two separate systems due to their differences in character, for example, average depth, amount of fresh water run-off, and overall size. In the current paper, we focus exclusively on the WDWS as a control area, but the analysis could be applied to any other multiple inlet system such as the EDWS.

2.2 Wind Characteristics

The wind characteristics at the mouth of the Texel inlet (4.7017° E, 52.9431° N) for the combined years 2009-2011 are shown in the wind rose depicted in Figure 2a. The data were obtained from the operational model of the German Weather Service (DWD) used to force the model, and have a spatial resolution of 1/16° and a temporal resolution of 3 h. For wind speeds smaller than 6 m s^{-1}, no clear preferential wind direction is observed, but winds with larger

Figure 2. Wind rose plot for the wind in the middle of the Texel Inlet. The plot represents the probability of occurrence (in %) per wind direction and speed range a) for the years 2009-2011, b) for the year 2009, c) for the year 2010, and d) for the year 2011. They are based on the atmospheric forcing data with a temporal resolution of 3 h. Colors indicate wind speed in m s^{-1}.

speeds—specially wind speeds larger than 10 m s^{-1}— are usually from the West to Southwest.

The wind characteristics have a considerable interannual variation, as illustrated for the years 2009–2011 (Figures 2b-d). The year 2010 was the calmest within the modelled period, and it did not present such a strong predominance of southwesterly winds as the other two years.

In the current paper, we use the times series of wind at the mouth of the Texel inlet to perform the analysis of the effect of wind in the residual volume transport. This station was chosen because it is located at the main tidal inlet which is also the best exposed to the preferential Westerly-Southwesterly winds, and moreover representative of the adjacent North Sea, with which water masses are exchanged. However, the effect of choosing a different station (e.g. a station located at the Vlie inlet, at the Terschelling watershed, and at the center of the WDWS) was also evaluated. It was found that the choice of the station does have an effect on some of the quantitative measures since the wind is not the same in different parts of the Wadden Sea. However, this effect is small and does not change the overall conclusions of the paper due to the small spatial variability of the wind. This variability was analyzed by comparing the time series at different locations, for example, at the mouth of the Texel inlet and at the Vlie inlet (5.1427° E, 53.3211° N). We performed a linear regression for both wind velocity components (East-West and North-South) resulting in slopes of 1.02 for the East-West component and 1.07 for the North-South component. The coefficient of determination between the two time series is $R^2 = 0.94$. This points are further addressed in Section 5.

3 Numerical Setup and computation of tidally averaged quantities

Three-dimensional numerical simulations of the hydrodynamics of the Dutch Wadden Sea, already described in detail by Duran-Matute et al. (2014), were used to calculate the current velocities. The simulations were performed using the General Estuarine Transport Model (GETM) with a horizontal resolution of 200 m and terrain following σ-coordinates with 30 layers in the vertical. At the open boundaries located in the North Sea (far enough from the inlets), the model was forced with realistic boundary conditions based on larger-scale oper-

ational models (meteorological forcing, tidal elevation and storm surges) and empirical data (freshwater discharge).

We extracted current velocity data at the transects across the inlets (Texel inlet, Eierlandse Gat, and Vlie Inlet) and at the Terschelling watershed shown in Figure 1. In addition, we extracted the instantaneous water volume as a function of time for the WDWS, i.e. in the area enclosed by the transects. All these data were exported with a temporal resolution of 30 min. As a convention, we consider the current velocities into the WDWS as positive, and outwards as negative.

GETM has a thin-layer flooding and drying algorithm. This means that at least a thin layer of fluid is always present in every grid cell. This algorithm depends on two parameters: the minimum depth D_{min} and the critical depth D_{crit}. The minimum depth D_{min} is the minimum thickness of the thin layer at any given grid cell, and D_{crit} is the thickness at which non-linear terms start being switched off giving rise to a balance between frictional forces and the pressure gradient force. For the simulations presented here, $D_{min} = 10$ cm and $D_{crit} = 26$ cm. We consider a grid cell to be dry if the depth is smaller than D_{crit}, although the exact value within some realistic bounds has little effect on the extent of the dry areas.

It has been previously shown that the model results compare well against several observational datasets: sea-level height at 14 different tidal gauges, salinity and temperature at one fixed station at the Texel inlet, and the instantaneous volume transport through the Texel inlet as measured by an acoustic Doppler current profiler (ADCP) beneath the TESO ferry covering the route from the port of Den Helder in the mainland to the island of Texel [*Duran-Matute et al.*, 2014]. A more detailed comparison between the model results and the results of the TESO ferry measurements was carried out by *Sassi et al.* [2015b], who also compared the residual volume transport through the Texel inlet. All these thorough comparisons with observations gives us confidence in using the simulations to study the residual volume transport in a realistic way.

The residual volume transport through an inlet is given by the integration over one tidal period of the instantaneous transport through that inlet. It is then crucial how the tidal period is defined *Duran-Matute and Gerkema* [see e.g. 2015]. Commonly it is defined as the time between two consecutive moments with similar conditions: low water, high water, slack tide going from ebb to flood, or slack tide going from flood to ebb. We define the tidal period as the time between two consecutive instants, taken during rising tides, when the instantaneous water volume inside the WDWS matches the long-term average value. This definition was first introduced by *Duran-Matute et al.* [2014], and its advantages were further discussed by *Duran-Matute and Gerkema* [2015].

Figure 3. a) Tidally averaged water volume inside the western Dutch Wadden Sea as a function of wind direction. The color denotes the wind speed. b) Water volume inside the western Dutch Wadden Sea as a function of the wind speed in the E-W direction. The red line in both plots denotes the average.

The tidal period as defined above was used to obtain time series, at tidal intervals, of the residual volume transport at every transect, the tidally averaged volume inside the WDWS, and the tidally averaged wind vector in the middle of the Texel Inlet for every tidal period within the years 2009-2011. In addition, the same definition was used to obtain maps and get spatial information of the tidally averaged sea level and vertically integrated volume transport at every grid cell during certain tidal periods.

4 Relationship of Wind Direction with Set-Up/Set-Down

Before studying the effect of wind on the residual volume transport through the system, we present results of the effect of wind on the tidally averaged volume inside the WDWS, which is directly related to the sea surface height. As it will be seen, this is relevant for the understanding of the relationship between the wind and the residual transport. Notice that the averaging over a tidal period smoothes extreme events, like a severe storm which usually lasts a few hours.

The volume inside the WDWS averaged per tidal period as a function of the wind direction is shown in Fig. 3a. The color denotes the wind speed. Clearly, the response of the volume inside the WDWS to wind is anisotropic: westerly winds favor set-ups, easterly winds favor set-downs, and Northerly and Southerly winds have little or no effect on the tidally averaged volume independently of their speed.

To further analyze the response of the system to the East-West component of the wind, we plot the tidally averaged volume inside the WDWS as a function of this component of the wind (Figure 3b). There is a non-linear response which is antisymmetric with respect to a 0 m s^{-1} wind speed. The scatter around the average volume must be due to factors such as the tidal conditions (spring-neap cycles, diurnal inequality, phase of the fortnightly and lower frequency tides, etc.), the temporal variation of the wind speed and direction within the tidal cycle, the sea level in the North Sea, and notably, the state of the system during the previous tidal cycle. In spite of the scatter, the effect of strong easterly and westerly winds is clearly visible.

The spatial structure of the wind induced set-ups and set-downs is illustrated through tidally averaged sea-level maps for some tidal periods with extreme wind conditions (Figure

Figure 4. Maps of tidally-averaged sea level for four distinct tidal periods with extreme average wind conditions: a) 13 m s^{-1} westerly wind, b) 13 m s^{-1} easterly wind, c) 12 m s^{-1} northwesterly wind and d) 16 m^{-1}s southwesterly wind.

4). We selected extreme conditions so that the effect of wind is the most visible. The drying of the tidal flats during part of the tidal period complicates the interpretation of this calculation, so we simply ignore any grid cell that is dry during some part of the tidal cycle. These grid cells are shown in white in Figure 4. For a tidal period with a strong (13 m s^{-1}) westerly average wind (Figure 4a), the sea level in the North Sea is already higher than MSL (about 0.9 to 1 m along the coast in the SW corner of the domain); inside the DWS, the sea level increases up to 1.3 m above MSL towards the closing dike and the coast in the southeast of the WDWS. For a tidal period with an average wind from the opposite direction with the same speed (Figure 4b), the average sea level in the North Sea is below MSL (about 50 cm along the coast in the SW corner of the domain); inside the DWS, there is a set-down of about 0.7 m close to the closing dike and the southwest corner of the WDWS. The large set-down clearly increases the exposure of the tidal flats. The spatial structure of the sea level for a strong northwesterly wind (Figure 4c) is similar to that of a strong westerly wind. A strong south-westerly wind (Figure 4d) generates a set-up with the highest water levels further shifted towards the Terschelling watershed. Comparing Figures 4a,c, and d), we can see an example of how westerly winds are more efficient in driving a setup than southwesterly and northerly winds. However, these figures seem to indicate that the difference already originates outside the Wadden Sea.

5 Effect of Wind on the Residual Volume Transport

5.1 The Effect at Each Inlet and the Watershed

The residual volume transport through the inlets delimiting the WDWS and for the Terschelling watershed was computed for every tidal period within the years 2009-2011. We studied its dependence on the wind speed and direction. Figure 5 shows the residual volume transport as a function of the tidally averaged wind direction. Positive transport means into the WDWS, and the color denotes the wind speed. The median residual transport is indicated with a horizontal white dashed line. It can be seen that the variability is much larger than the median since the median of the residual volume transport is in the order of a few hundred m^3 s^{-1} while the full range of variability is two orders of magnitude larger, about 25000 m^3 s^{-1} (Figure 5a).

Figure 5. Scatter plots of wind direction vs. residual volume transport for each tidal period within the years 2009-2011 for a) the Texel Inlet, b) the Eierlandse Gat, c) the Vlie Inlet, and d) the Terschelling watershed. The color denotes the wind speed (m s^{-1}). The white dashed line corresponds to the median residual volume transport for the three year period.

The largest residual volume transport across the different transects occurs for large wind speeds but only from specific wind directions. In other words, the response of the residual volume transport to the wind is anisotropic. For all transects, we observe two preferential directions: one for inflows and one for outflows. For the Texel inlet, for example, the largest inflows occur during strong southwesterly winds, while outflows occur during strong northerly winds, and for the Vlie inlet, the picture is reversed. Just as there are wind directions favoring large residual currents, there are also wind directions that have little to no effect on the residual volume transport even when the wind is strong. We shall refer to these directions as "passive" directions.

In the plots shown in Figure 5, there is a lack of symmetry between the two preferential wind directions for each of the transects n two ways: (1) the preferential wind directions forcing large inflows and outflows are not necessarily opposite to each other, and (2) the magnitude of the residual volume transport is usually larger for one of the preferential wind directions. There is of course the anisotropy in the wind rose itself (Figure 2) with its prevailing winds from the Southwest that can mask the relationship between the residual volume transport and the wind in Figure 5.

To unmask this relationship and quantify the sensitivity of the residual volume transport to wind, we assume that the residual transport is proportional to the wind stress $\vec{\tau_w}$. This is a priori true if all other forcing mechanisms are neglected [*Nihoul and Ronday*, 1975; *Buijsman and Ridderinkhof*, 2007]. The residual volume transport Q_0 through an inlet is a linear function of the wind stress $\vec{\tau_w}$, i.e. of $|\vec{w}|\vec{w}$, where $\vec{w}$ is the wind vector. We consider for our analysis that the residual volume transport depends on the wind direction θ and the wind speed w such that

$$Q_0(\theta) \sim K(\theta)w^2 + B, \tag{1}$$

where $K(\theta)$ can be interpreted as the conductance (the inverse of the resistance) of a wind-driven residual through-flow, and we assume that it depends on wind direction θ. The constant B in eq. (1) represents the average residual volume transport during weak wind conditions: due to the tides, fresh water discharge, and baroclinic effects. We compute B for every inlet

Figure 6. Conductance K of the residual volume transport to the wind (solid blue line) at each transect as a function of the wind direction θ. The dashed lines represent the 95% confidence interval (CI). The green dotted line represents the correlation coefficient of the linear fit for each wind direction.

by taking the average of the residual volume transport for tidal periods with an average wind speed smaller than 2 m s^{-1} (there is not a significant difference if the limit is slightly increased).

To calculate $K(\theta)$, we first sort the tidal periods into bins defined by the tidally average wind direction θ. The bins span 10° from $\theta - 10.0^\circ$ to $\theta + 10.0^\circ$ where θ goes from 0° to 360° in 10° intervals. The intervals were chosen ad hoc so that all of them have large enough number of tidal periods to have reliable statistics. A curve of the form given by eq. (1) is fitted using *least squares* to the residual volume transport Q_0 as a function of w^2 . Figure 6 shows the resulting values of K [with a 95% confidence interval (CI)] and the corresponding values of the correlation coefficient R as a function of the wind direction for the four transects. The angle corresponding to the maximum of K is then the inherent preferential direction for inflows, and the angle corresponding to the minimum of K is the preferential direction for outflows. The crossings of K through zero correspond to the passive directions. Note that the absolute value of the correlation coefficient is close to unity, except, obviously, in the vicinity of a passive direction. This supports the assertion that wind is the main driving mechanism. In addition, the span of the 95% CI is in general small compared to the variations in the value of K.

The 95% CI interval is determined from the fit. However, the exact value of K can be affected by the choice station for the wind time series, and the values of the model parameters (D_{crit}, D_{min}, and the bottom roughness length z_0 [see e.g. *Herrling and Winter*, 2015]) which influence the computed residual volume transport. Nonetheless, the effect of the choice in wind station is limited due to the small spatial variability of the wind within the region and it does not change Figure 6 qualitatively. Due to the overall good comparison with observations, we believe the estimates of the residual volume transport to be accurate. A better sense of this accuracy could be obtained only by the comparison with more observations (for example, salinity on both sides of the Terschelling watershed), which are lacking.

From this analysis, we can conclude that the Texel Inlet has the largest conductance K, and it is followed by the Vlie Inlet and the Terschelling watershed almost tied in second place. The Eirlandse Gat has clearly the lowest conductance. Due to the large connectivity between the Texel and Vlie inlets, their efficiency is almost mirrored: a wind-driven inflow through the Texel Inlet translates into an outflow through the Vlie Inlet and vice versa. Notice that the largest

Figure 7. Relative contribution of each transect (in %) to the total residual volume transport through the system as a function of wind direction. Positive values mean a contribution to the inflow and negative values to the outflow.

conductance for inflows at the Texel Inlet and for outflows at the Vlie Inlet corresponds to winds coming almost from the South, and not from the South-West as it seemed from Fig. 5. This difference can be attributed to the anisotropy of the wind rose which plays a role in Fig. 5 but not in Fig. 6.

For the Eierlandse Gat and the Terschelling watershed the preferential directions tend to be more aligned with the East-West direction. This is probably due to the relative orientation of these transects, but also the higher water levels during winds along this direction that allow for water to be transported more easily through the shallow tidal flats.

Due to continuity, the sum of K for the four transects at each wind direction tends to zero (within an error margin of about 10 %). This allows us to easily calculate for any given wind direction the relative contribution of each inlet to the total residual volume transport through the whole system (i.e. the volume of water that passes through the WDWS within one tidal cycle). For example, during a Southerly wind 100% of the inflow is through the Texel Inlet, while the ouflow spreads 78% through the Vlie Inlet and 32% through the Terschelling watershed, with a negligible flow through the Eierlandse Gat. The relative contribution of each transect (in percentage) to the total residual volume transport through the system as a function of the wind direction is shown in Fig. 7.

Figure 8 shows the residual volume transport as a function of the wind speed for the preferential directions of all four transects and the corresponding fits (an overview is given in Table 1). As can be seen from the figure, and the values for the root-mean-square (rms) error and the correlation coefficient, the fits give an accurate estimate of the residual volume transport. The plots in Fig. 8 also include the limits of the 95% CI that is given by the curves:

$$(K(\theta) \pm S_K)w^2 + (B \pm 2\sigma_B) \tag{2}$$

with σ_B the standard deviation of B and S_K the standard error of K. However, the error in K is relatively small and most of the variability is explained by the standard deviation of B. This suggests that the reasons behind the scatter are the same for any value of w, and these are, mainly, the fresh water discharge, the variability in the tides, baroclinic effects, and large scale variability in the North Sea.

Table 1. Overview of the preferential directions for all the transects: conductance K, residual volume transport during weak wind conditions B, correlation coefficient R, and root-mean-square (rms) error.

Transect	outflow/ inflow	preferential wind direction	K (m s)	B (m^3 s^{-1})	R	rms error (m^3 s^{-1})
Texel Inlet	inflow	190°	64	-837	0.84	1244
	outflow	10°	-45	-837	-0.89	756
Vlie Inlet	inflow	340°	27	728	0.72	717
	outflow	190°	-46	728	-0.85	1070
Eierlandse Gat	inflow	280°	16	-232	0.87	368
	outflow	140°	-9	-232	-0.69	216
Terschelling watershed	inflow	20°	20	-49	-0.89	310
	outflow	260°	-37	-49	-0.90	636

Figure 8. Scatter plots of wind speed vs. residual volume transport for each tidal period within the years 2009-2011 with the wind blowing from both preferential directions ($\pm 10°$) for a) the Texel Inlet, b) the Eierlandse Gat, c) the Vlie Inlet, and d) the Terschelling watershed. The blue color corresponds to the preferential direction for inflows, while the green color corresponds to the preferential direction for outflows. The solid lines correspond to fits of the function given in equation (1) and the dashed lines represent the 95% CI.

The value of the parameter B (given in Table 1) is an indication of the residual volume transport during periods of weak winds. Its values suggest that the tides and the fresh water discharge usually drive a residual circulation with an inflow through the Vlie Inlet and an outflow through the Texel Inlet, Eierlandse Gat, and the Terschelling watershed. The actual values are similar to those obtained by *Ridderinkhof* [1988a] with 2D simulations that included only tides as forcing. In our simulations, we obtain a weaker inflow through the Vlie inlet with a difference of 417 m^3 s^{-1} which is probably due to the extra outflow of fresh water which is in the order of 400 m^3 s^{-1}.

5.2 Spatial Patterns of Residual Flows

The spatial structure of the residual volume transport in the WDWS is studied by computing the tidally averaged residual transport at every grid cell in the domain. Although the definition of the tidal period is based on the area enclosed by the four transects shown in Figure 1, the residual transport outside this area is also presented for illustration purposes. Figure 9 shows the residual transport stream-lines for six different tidal periods. The first two correspond to periods with weak winds, and the last four correspond to the same extreme peri-

Figure 9. Residual circulation for six tidal periods with different wind conditions: a) 2 m s^{-1} easterly wind, b) 6 m s^{-1} southwesterly wind, c) 13 m s^{-1} westerly wind, d) 13 m s^{-1} easterly wind, e) 16 m s^{-1} southwesterly wind, and f) 12 m s^{-1} northwesterly wind. The residual circulation is illustrated with transport stream lines. The color denotes the magnitude of the transport (yellow stronger, red weaker). The grey scale in the background represents the bathymetry.

ods used to illustrate the spatial structure of set-ups and set-downs in Figure 4. Again, we chose extreme conditions that accentuate the characteristic patterns.

For very weak winds, recirculation cells dominate the spatial patterns. This is in agreement with earlier studies on residual circulation due to tidal flow over topography [*Loder*, 1980; *Zimmerman*, 1981] and related numerical studies [*Ridderinkhof*, 1988a]. Note that these studies neglected wind effects. For stronger winds (Figure 9c-f), the spatial patterns show more large-scale coherence to the point that the smaller recirculation cells may disappear completely (e.g. Figure 9f). These figures show the spatial representation of the residual transport associated with the results on the preferential directions discussed previously. The radical change in the residual-flow patterns, brought about by changes in wind strength and direction, is also likely to have implications for the phenomenon of chaotic stirring [*Zimmerman*, 1986], which depends on the combination of (Eulerian) tidal and residual flows causing complicated and chaotic trajectories for particles (the Lagrangian view).

For a strong easterly wind (Figure 9d), the residual circulation is weak. In particular, the set-down limits the transport through the Terschelling watershed and through the watersheds isolating the Eierlandse Gat from the rest of the WDWS. In these circumstances, transports across these watersheds can occur only during a short fraction of the tidal period, when the sea level is high enough.

Strong south to southwesterly winds (Figure 9f) force the largest residual transports. These winds are aligned with the geographical orientation of the system and force a strong inflow through the Texel inlet and an outflow through the Vlie Inlet and the Terschelling watershed. In this case, the set-up at the Terschelling watershed facilitates the flow through it.

In general, it can be said that the response of the residual transport to wind is highly dependent on the topography, i.e. the relative orientation of the inlets, the orientation of the channels, and the connectivity between the inlets (that can also be modified due to wind set-ups and set-downs).

Figure 10. a) Scatter plot of wind direction vs. sum of the residual volume transport into the system for each tidal period within the years 2009-2011. The color denotes the wind speed. b) Conductance K of the residual volume transport through the system as a function of wind direction (solid blue line). The 95% CI is given by the dashed blue lines. The dotted green line represents the correlation coefficient R of the linear regression.

Figure 11. Cumulative volume transported through the three inlets, the Terschelling watershed, and the sluices starting on 1 January 2009.

6 Effect of Wind on the Total Residual Volume Transport

6.1 Effect of Wind on a Short Time Scale (One Tidal Period)

One of the advantages of the definition of the tidal period used to calculate the residual volume transport is that we obtained automatically a closed balance: the sum of the residual volume transport at all the transects, the rate of fresh water discharge, evaporation rate and precipitation equals zero [*Duran-Matute and Gerkema*, 2015]. In this way, the magnitude of the total residual volume transport through the system for a given tidal period can be obtained by adding all the *inflows* or all the outflows through the inlets. Here we consider the sum of all the inflows which in fact disregards the fresh water discharged into the system. However, this is sensible since the discharge does not depend on the magnitude of the wind.

Figure 10a) shows the total tidally averaged inflow into the system as a function of the tidally averaged wind direction. As for the individual transects, winds from certain directions have a strong effect, while from some others, wind barely affects the residual volume transport. Figure 10b) shows the total conductance of the system as a whole, K, as a function of wind direction. The largest values for the residual volume transport occur during strong southwesterly winds (Figure 10b), the main wind direction for the largest storms in the region, but the largest conductance K of the system is to Southerly and Northerly winds. The system has the lowest conductance during winds from land (i.e. Easterly/Southeasterly winds) as could be expected since no water can be dragged from that direction.

6.2 Effect of Wind on the Long-Term State of the System

The long term cumulative volume of water transported into the WDWS through the sluices, the three inlets, and the Terschelling watershed presents, in general, a linear behavior (Fig. 11). However, this trend is modified seasonally. For example, more water is discharged through the sluices during the autumn and winter months than during the spring and summer months.

Table 2. Long-term residual volume transport obtained through a linear fit through the cumulative volume shown in Figure 11.

	slope (m^3 s^{-1})
Texel Inlet	-363
Vlie Inlet	473
Eierlandse Gat	-66
Terschelling watershed	-541
Fresh water	457

For the case of the Texel inlet, the typical outward linear trend can be upset during autumn and winter months. This is particularly clear at the end of 2009 and 2011, when there were strong storms with southwesterly winds. To estimate the magnitude of the long term residual volume transport, we have fitted a line to each of the curves in Fig. 11. The slope of these lines (shown in Table 2) gives an estimate of the long-term residual volume transport through the inlets. For the water from the sluices, the slope is equivalent to the average discharge ($\sim$ 450 m^3 s^{-1}). For the Texel and the Vlie inlets, the slope suggests that the long-term residual volume transport is weaker than the average during weak wind conditions given by the value of B in Table 1. In contrast, the long-term residual volume transport through the Terschelling watershed is larger than the average during weak wind conditions. This difference is due to the wind since it opposes the tidally driven flow going from the Vlie inlet to the Texel inlet, but facilitates the flow through the Terschelling watershed. These results indicate that the wind-driven residual volume transport not only overshadows the tidally-driven volume transport during strong wind events, but that these events crucially stamp the long-term mean (trend) as well.

Here we have looked at the residual flow of water and the role of wind at the different inlets and the Terschelling watershed. For the residual transport of sediment, pollutants, nutrients and fresh water (which are usually of higher environmental importance), one can proceed similarly and apply the same techniques to quantify the response to wind direction/strength. Figure 12 shows the cumulative transport of fresh water through the three inlets and the watershed. For all four transects, there is a distinct seasonal signature due to the fact that the storms with strong southwesterly winds occur usually during the autumn and winter months. This gives the curve of the transport through the watershed a clear staircase shape: during periods of calms wind, there is no outflow of fresh water, and during periods of frequent strong southwesterly winds, there is a clear outflow.

Figure 12. Cumulative volume of fresh water from the sluices at Den Oever and Kornwerderzand flowing out through the inlets and the Terschelling watershed starting on 1 January 2009.

7 Conclusions

We performed a thorough analysis of the effect of the wind on the tidally averaged residual volume transport in the western Dutch Wadden Sea — a multiple-inlet system — through realistic three-dimensional baroclinic numerical simulations. The length of the simulations (three years) allowed us to study the effect of the wind in a large variety of conditions, and hence understand and quantify its overall effect in the residual volume transport through the system.

The residual transport at each inlet displays a particular response to the wind that can be quantified by computing its conductance as a function of the wind direction. The conductance at each inlet depends, in general, on the bathymetry, i.e. the overall geometry of the basin, the relative position of the inlet, the size of the inlet, and the connectivity between the inlets. However, we observe certain general characteristics: 1) the wind is responsible for most of the variability of the residual volume transport through the inlets and, 2) the response of the residual volume transport at each inlet is anisotropic, i.e. it has two preferential directions (one for inflows and one for outflows) and two passive directions associated with it.

In spite of the different behavior of individual inlets, it is possible to quantify the conductance for wind-driven residual volume transport through the system as a whole. In the particular case of the western Dutch Wadden Sea, the direction with the highest conductance of the system is close to the dominant wind direction in the region. This favors strong flushing episodes with an inflow through the Texel inlet and an outflow through the Vlie inlet and the Terschelling watershed during strong winds from the South to Southwest (i.e. from the preferential direction of the system). Although the strong winds due to storms are episodic, they have a marked effect in the longer term (e.g. seasonal, yearly) statistics of the residual circulation in the system.

The analysis presented here also shows that the character as a barrier between the WDWS and the EDWS of the Terschelling watershed is completely lost during strong winds from the associated preferential directions. Due to the dominant Westerly and Southwesterly winds, there is then a net large residual volume transport from the western to the eastern Dutch Wadden Sea .

The conclusions outlined above for the net transport of water can also be extended to the transport of other quantities such as sediment [see e.g. *Sassi et al.*, 2015a] and fresh wa-

ter which have more environmental importance. However, in these cases other factors such as the availability and the position of the sources also play a role.

In the face of climate change, that could produce changes in global wind patterns or on the frequency and intensity of storms, the results presented in the current paper suggest an important modification of the overall flushing and residual volume transport through the western Dutch Wadden Sea if such scenarios become a reality. This modification can be quantified for concrete possible wind scenarios using the effective conductance of the system K for the wind-driven residual volume transport computed in the current paper.

Acknowledgments

We thank all participants in the PACE project for inspiring discussions, in particular Hans Burchard. The authors would like to thank Giordano Lipari for useful discussions. This project was funded by the NWO-ZKO/BMBF bilateral project "The future of the Wadden Sea sediment fluxes: still keeping pace with sea level rise?" (NWO-ZKO #839.11.003). The times series used for all the calculations in this paper are available upon request.

References

Bellafiore, D., G. Umgiesser, and A. Cucco (2008), Modeling the water exchanges between the Venice Lagoon and the Adriatic Sea, *Ocean Dynam.*, *58*(5-6), 397–413, doi:10.1007/s10236-008-0152-7.

Buijsman, M. C., and H. Ridderinkhof (2007), Water transport at subtidal frequencies in the Marsdiep inlet, *J. Sea Res.*, *58*(4), 255–268, doi:10.1016/j.seares.2007.04.002.

Duran-Matute, M., and T. Gerkema (2015), Calculating residual flows through a multiple-inlet system : the conundrum of the tidal period, *Ocean Dynam.*, *65*(11), 1461–1475, doi:10.1007/s10236-015-0875-1.

Duran-Matute, M., T. Gerkema, G. J. de Boer, J. J. Nauw, and U. Gräwe (2014), Residual circulation and freshwater transport in the Dutch Wadden Sea: a numerical modelling study, *Ocean Sci.*, *10*(4), 611–632, doi:10.5194/os-10-611-2014.

Farinha Fabiao, Joao Pedro and M. F. Gomez Rodrigues, and A. B. Fortunato and J. M. Quintela de Brito Jabob and A. M. Francisco Cravo (2016), Water exchanges between a multi-inlet lagoon and the ocean: the role of forcing mechanisms, *Ocean Dynam.*, *66*, 173–194,doi:10.1007/s10236-015-0918-7.

Gerkema, T. and J. J. Nauw and C. M. van der Hout (2014), Measurements on the transport of suspended particulate matter in the Vlie Inlet, *Neth. J. Geoscin.*, *93*(3), 95–105, doi:10.1017/njg.2014.7.

Herrling, G., and Winter, C. (2015), Tidally- and wind-driven residual circulation at the multiple-inlet system East Frisian Wadden Sea, *Cont. Shelf Res.*, *106*, 45–59, doi: 10.1016/j.csr.2015.06.001.

Jia, P., and Li, M. (2012), Dynamcs of wind-driven circulation in a shallow lagoon with strong horizontal density gradient, *J. Geophys. Res.-Oceans*, *117*, C05013, doi: 10.1029/2011JC007475.

van de Kreeke, J. (1976), Tide-induced mass transport; a flushing mechanism for shallow lagoons, *J. Hydraul. Res.*, *14*(1), 61–67, doi:10.1080/00221687609499688.

van de Kreeke, J., and D. Cotter (1974), Tide-induced mass transport in lagoon-inlet systems, *Coast. Eng.*, pp. 2290–2301.

Li, C. (2013), Subtidal water flux through a multiple-inlet system: Observations before and during a cold front event and numerical experiments, *J. Geophys. Res.-Oceans*, *118*(4), 1877–1892, doi:10.1002/jgrc.20149.

Liu, J. T., and D. G. Aubrey (1993), *Tidal Residual Currents and Sediment Transport Through Multiple Tidal Inlets*. In: D. G. Aubrey and G. S. Giese (eds.), *Formation and Evolution of Multiple Tidal Inlets, Coastal and Estuarine Studies*, v.44, American Geophysical Union, doi:10.1029/CE044p0113.

Loder, J. (1980), Topographic rectification of tidal currents on the sides of Georges Bank, *J. Phys. Oceanogr.*, *10*(4), 1399–1416.

Louters, T., and F. Gerritsen (1994), Het mysterie van de wadden: Hoe een getijdesysteem inspeelt op de zeespiegelstijging, *Tech. rep.*, Ministerie van Verkeer en Waterstaat, Directoraat-Generaal Rijkswaterstaat, Rijksinstituut voor Kust and Zee (RIKZ), The Hague.

Meyers, S. D., M. E. Luther, M. Wilson, H. Havens, A. Linville, and K. Sopkin (2007), A numerical simulation of residual circulation in Tampa Bay. Part I: Low-frequency temporal variation, *Estuar. Coast.*, *30*(4), 679–697, doi:10.1016/j.seares.2013.11.013.

Nauw, J., L. Merckelbach, H. Ridderinkhof, and H. van Aken (2014), Long-term ferry-based observations of the suspended sediment fluxes through the marsdiep inlet using acoustic doppler current profilers, *J. Sea Res.*, *87*(0), 17 – 29, doi:10.1007/BF02841965.

Nihoul, J. C. J. and F. C. Ronday (1975), The influence of the "tidal stress" on the residual circulation Application to the Southern Bight of the North Sea, *Tellus*, *27*(5), 484–489.

Ridderinkhof, H. (1988a), Tidal and residual flows in the western Dutch Wadden Sea I: numerical model results, *Neth. J. Sea Res.*, *22*(21), 1–21.

Ridderinkhof, H. (1988b), Tidal and residual flows in the Western Dutch Wadden Sea II: an analytical model to study the constant flow between connected tidal basins, *Neth. J.*

Sea Res., *22*(22), 185–198.

Salles, P., G. Voulgaris, and D. G. Aubrey (2005), Contribution of nonlinear mechanisms in the persistence of multiple tidal inlet systems, *Estuar. Coast. Shelf S.*, *65*(3), 475–491, doi:10.1016/j.ecss.2005.06.018.

Salles, P., A. Valle-Levinson, A. Sottolichio, and N. Senechal (2015), Wind-driven modifications to the residual circulation in an ebb-tidal delta: Arcachon lagoon, southwestern france, *J. Geophys. Res.-Oceans*, *120*(2), 728–740, doi:10.1002/2014JC010311.

Sassi, M. G., T. Gerkema, M. Duran-Matute, and J. J. Nauw (2015a), Residual water transport in the Marsdiep tidal inlet inferred from observations and a numerical model, *in press in J. Mar. Res.*, pp. 1–29.

Sassi, M. G., M. Duran-Matute, T. van Kessel, and T. Gerkema (2015b), Variability of residual fluxes of suspended sediment in a multiple tidal-inlet system: the Dutch Wadden Sea, *Ocean Dynam.*, *65*(9), 1321–1333, doi:10.1007/s10236-015-0866-2.

Smith, N. (1990), *Wind domination of residual tidal transport in a coastal lagoon*, pp. 123–133, Springer-Verlag, New York.

Smits, A., A. M. G. Klein Tank, and G. P. Können (2005), Trends in storminess over the Netherlands, 1962-2002, Int. J. Climatol., *25*(10), 1331–1344 doi:10.1002/joc.1195.

Stanev, E. V., J.-O. Wolff, H. Burchard, K. Bolding, and G. Flöser (2003), On the circulation in the East Frisian Wadden Sea: numerical modeling and data analysis, *Ocean Dynam.*, *53*(1), 27–51, doi:10.1007/s10236-002-0022-7.

Waterhouse, A. F., B. Tutak, A. Valle-Levinson, and Y. P. Sheng (2013), Influence of two tropical storms on the residual flow in a subtropical tidal inlet, *Estuar. Coast.*, *36*, 1037–1053, doi:10.1007/s12237-013-9606-3.

Weisse, R., H. von Storch, H. D. Niemeyer, and H. Knaack (2012), Changing North Sea storm surge climate: An increasing hazard?, *Ocean Coast. Manage.*, *68*, 58–68, doi:10.1016/j.ocecoaman.2011.09.005.

Zimmerman, J. T. F. Z. (1981), Dynamics, diffusion and geomorphological significance of tidal residual eddies, *Nature*, *209*, 549–555.

Zimmerman, J. T. F. Z. (1986), The tidal whirpool: a review of horizontal dispersion by tidal and residual currents, *Neth. J. Sea Res.*, *20*(2/3), 133–154.

Figure 1.

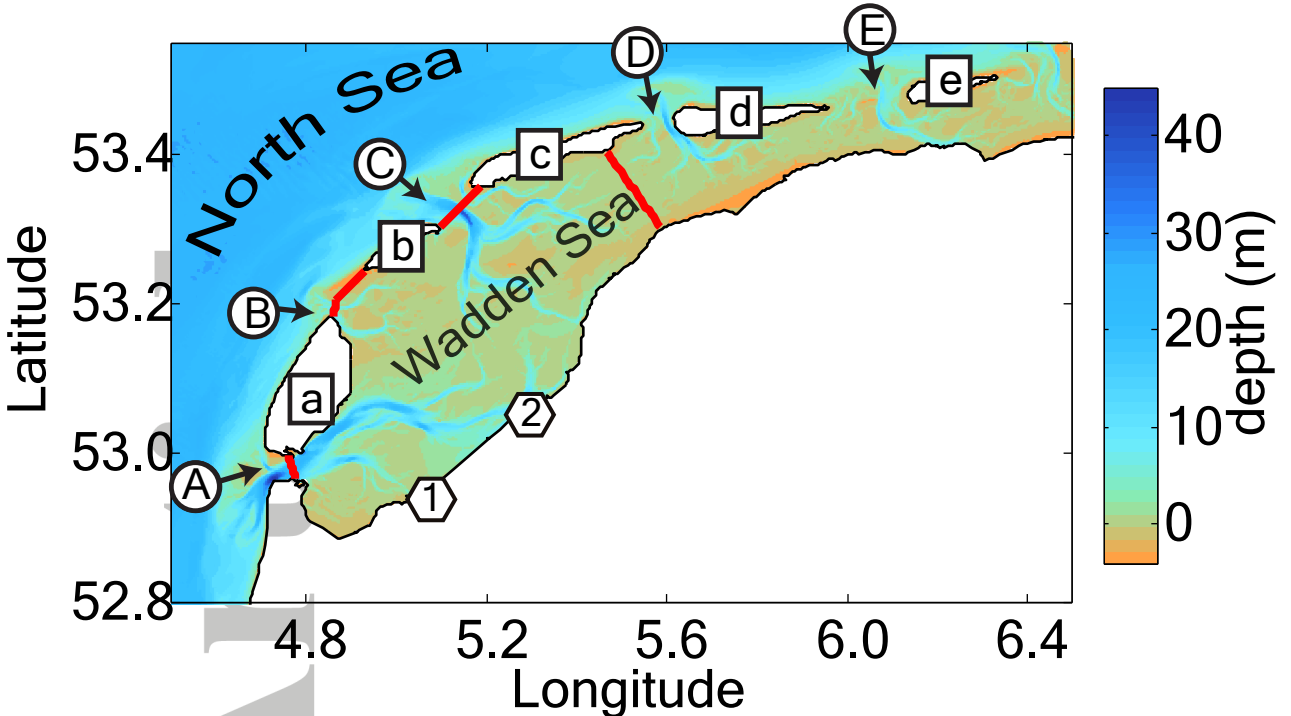

Islands
- a Texel
- b Vlieland
- c Terschelling
- d Ameland
- e Schiermonnikoog

Inlets
- A Texel Inlet
- B Eierlandse Gat
- C Vlie Inlet
- D Borndiep
- E Friesche Inlet – Pinkegat

Main sluices
- 1 Den Oever
- 2 Kornwerderzand

Figure 2.

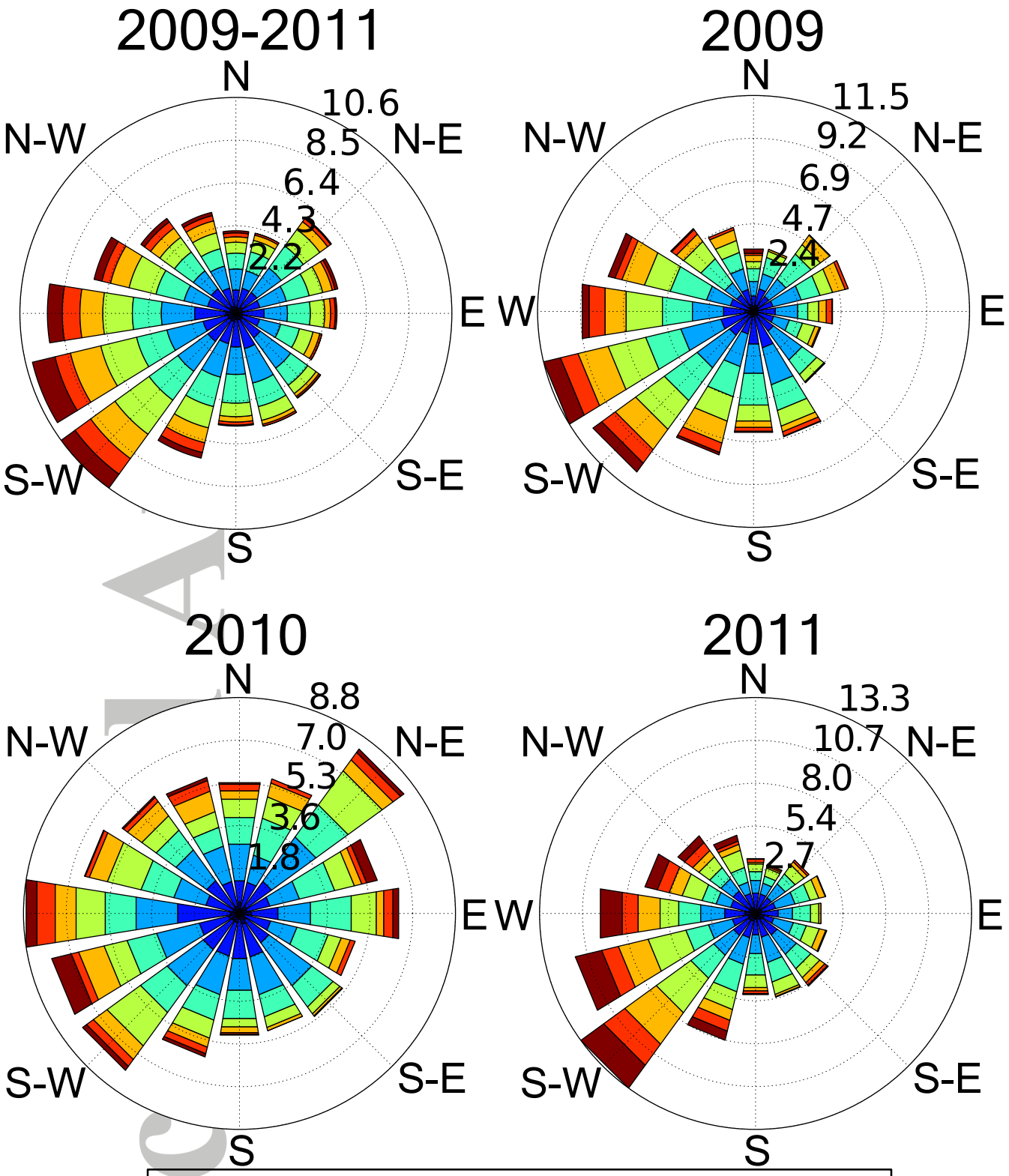

Figure 3.

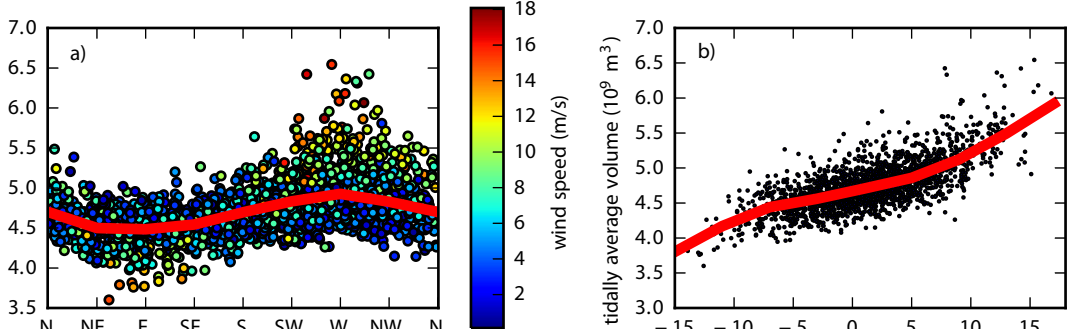

Figure 4.

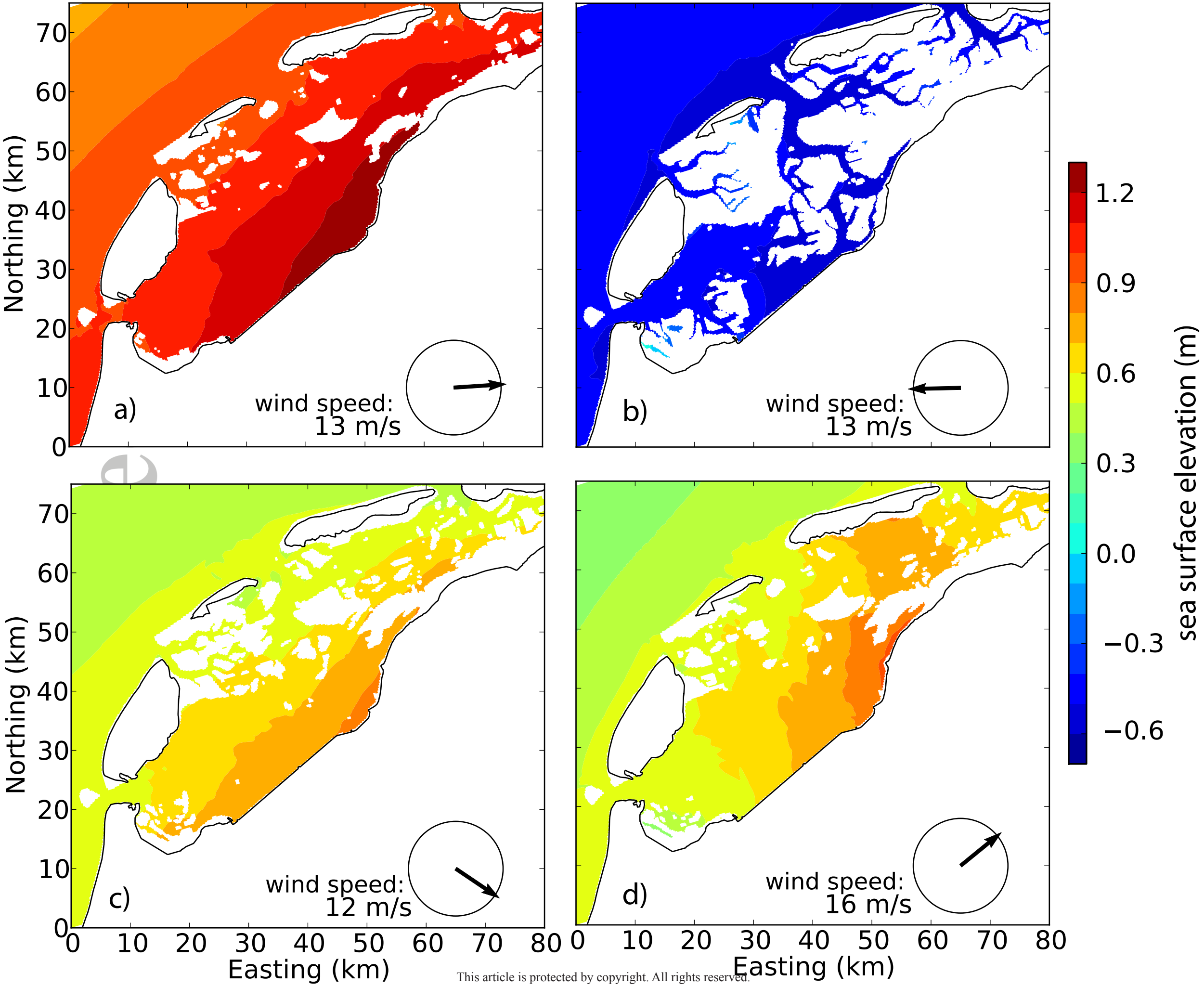

Figure 5.

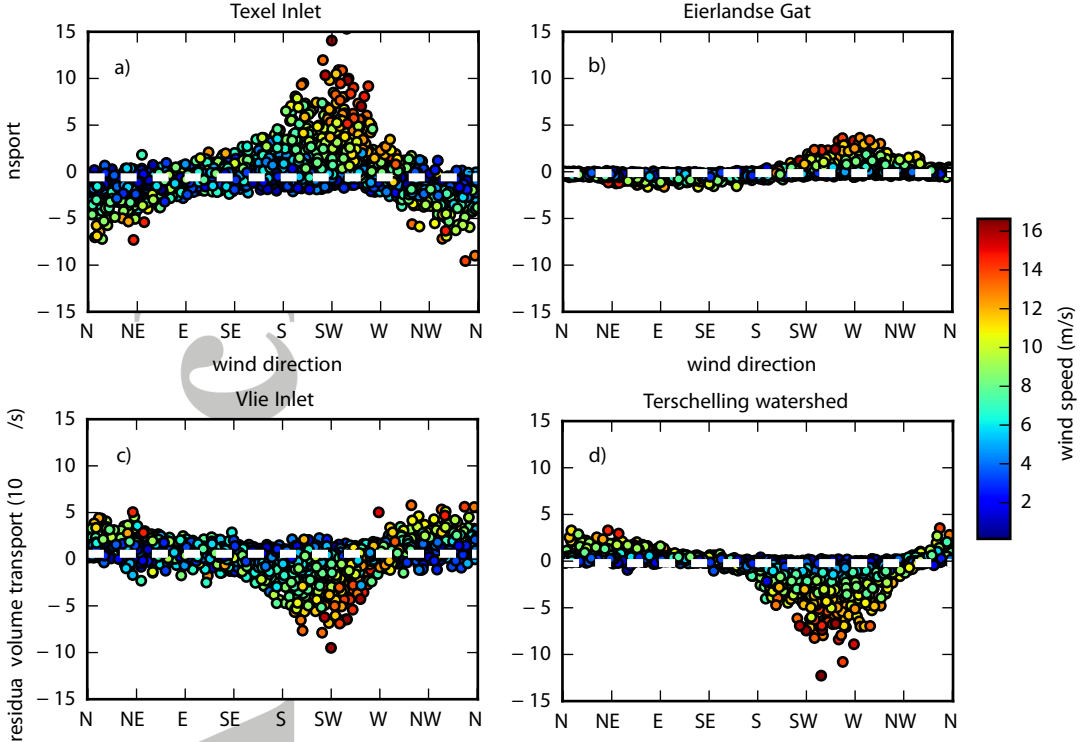

Figure 6.

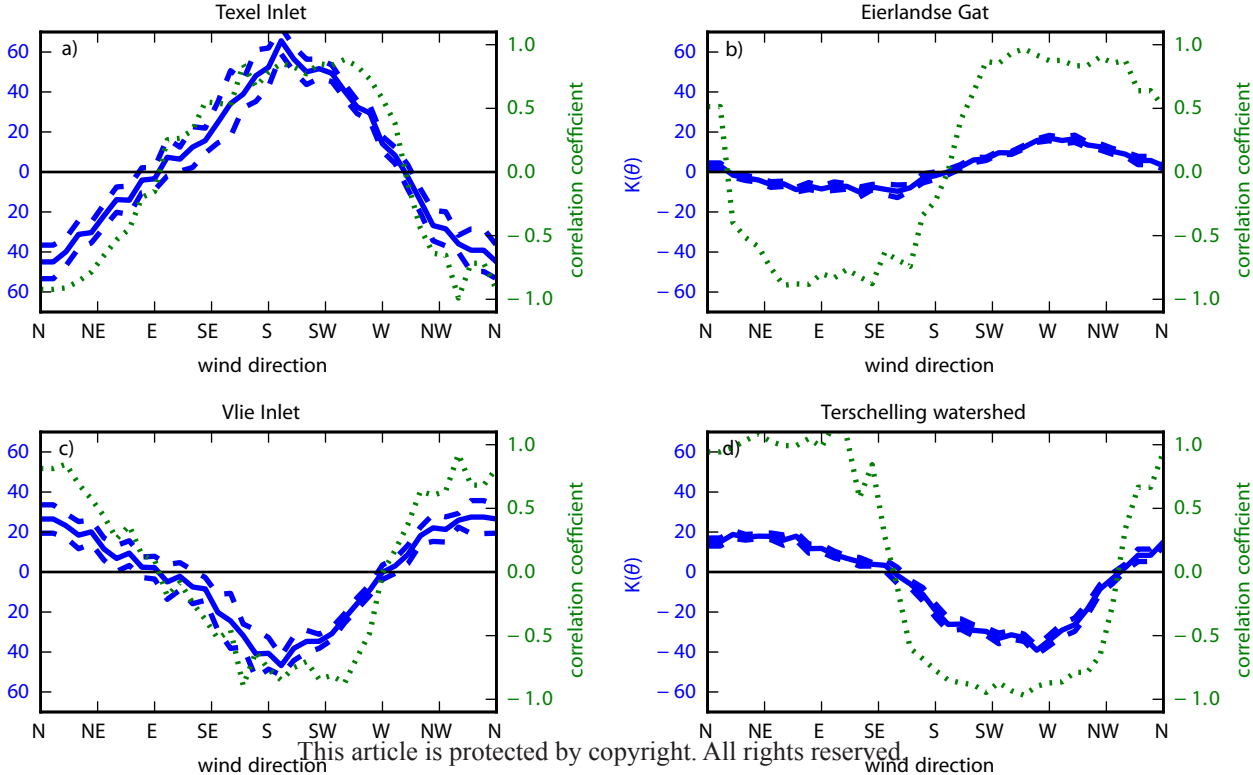

Figure 7.

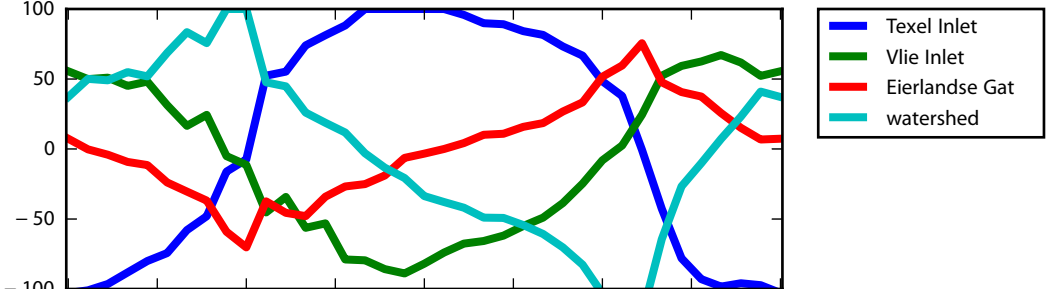

Figure 8.

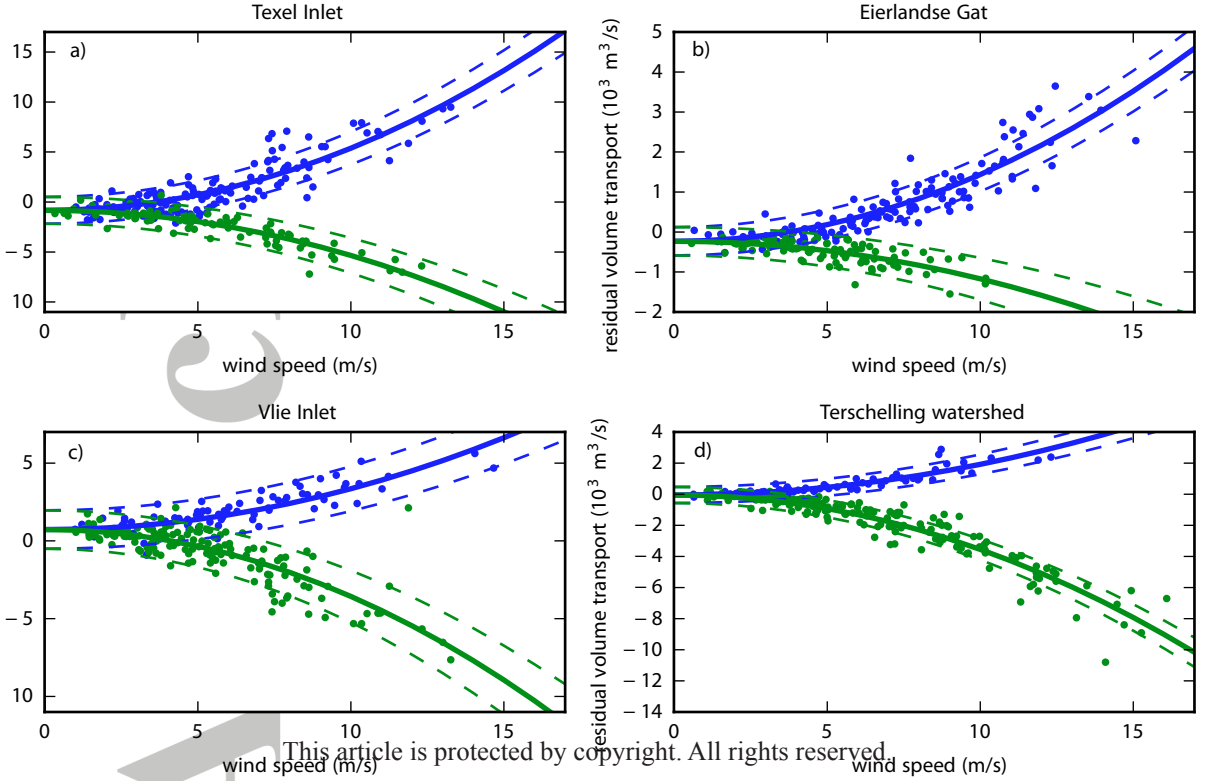

Figure 9.

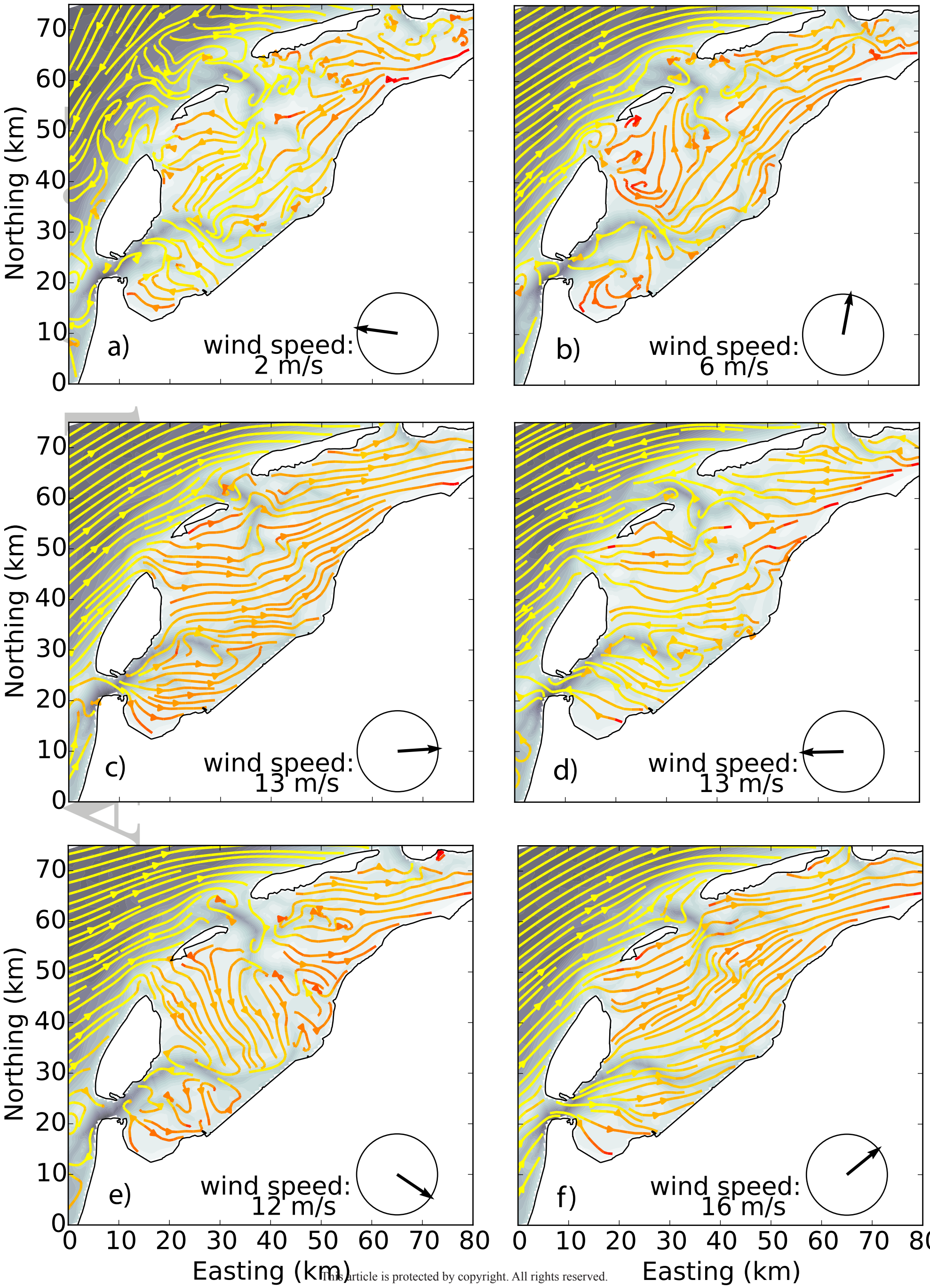

Figure 10 Corrected.

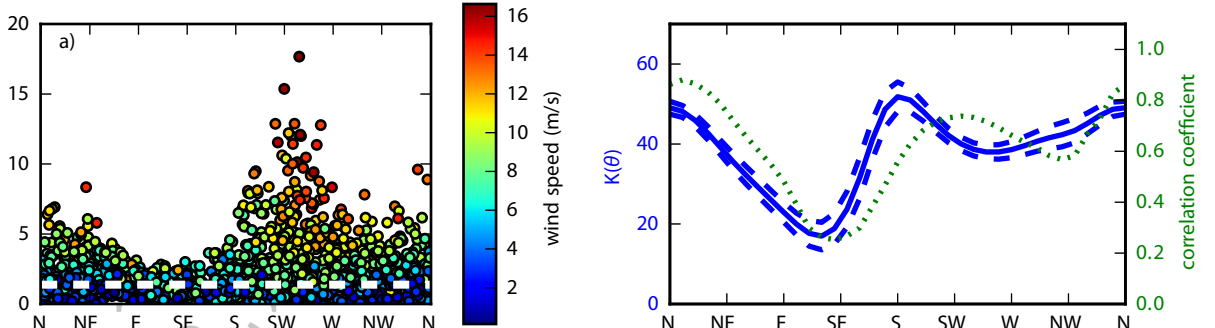

Figure 11 Corrected.

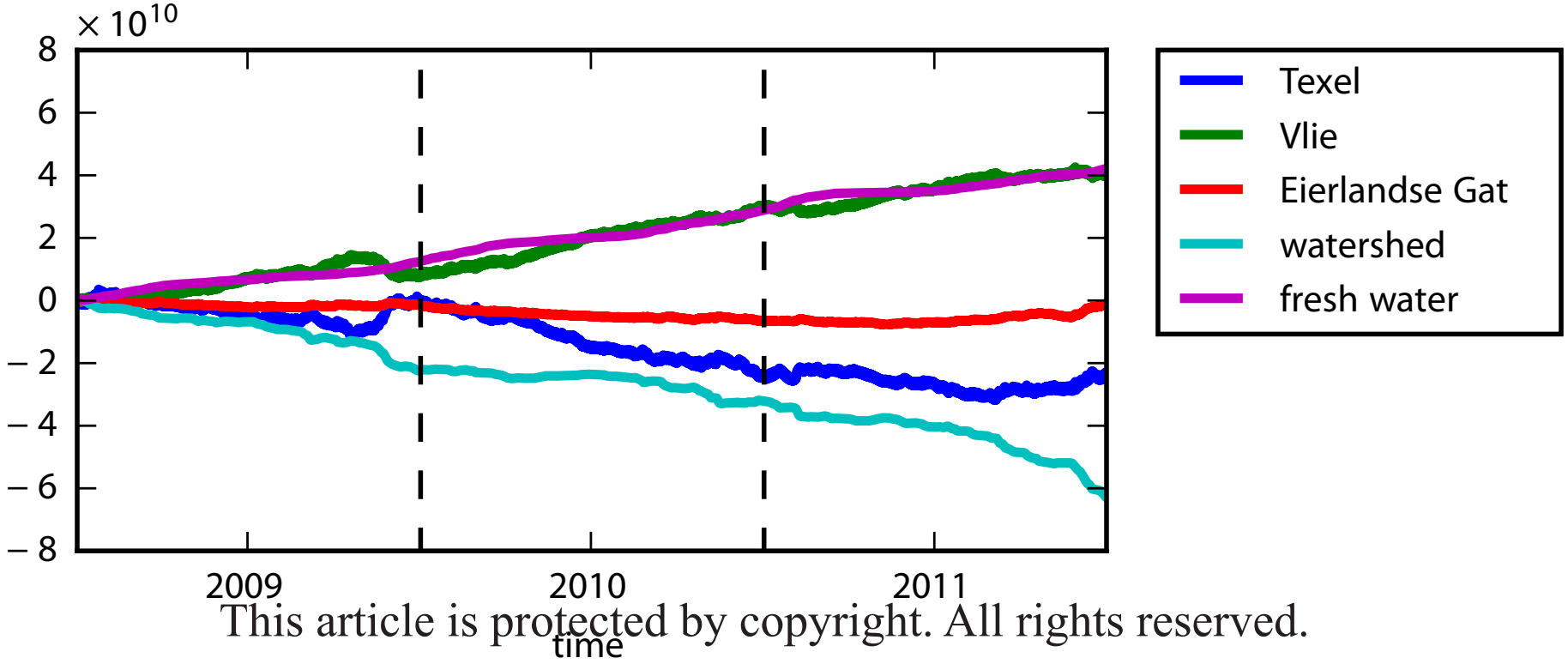

Figure 12 Corrected. Figure 12 Corrected